AN EXPERIMENTAL STUDY OF THE MICROSTRUCTURAL MECHANISM INFLUENCING CRACK CLOSURE STRESSES IN A FINE-SAND MORTAR

R. Dasgupta, J.C. Hay, J. McConnell and K.W.White,
Department of Mechanical Engineering, University of Houston, Houston, USA

C.Vipulanandan,
Department of Civil and Environmental Engineering, University of Houston, Houston, USA

Abstract

The post-fracture tensile (PFT) technique is well established in the studies of wake toughened ceramic systems. Through this experimental procedure, regions responsible for crack closure stresses are isolated and characterized, providing the constitutive stress-displacement relationship unique to the microstructure. This technique when applied to cementitious materials will offer a unique perspective to assess the effectiveness of sand grain morphology and size distribution.

A mortar consisting of rounded sand grains ranging from 0.1 to 1.4 mm in diameter and cement provides baseline data for wake toughening properties in a cementitious material study. Using the grain-size distribution and experimental stress-displacement results, we estimate that this rounded sand morphology effectively supports loads over a crack opening displacement (COD) of 1/15th the grain size.

Introduction

Recent attention in the fracture mechanics of cementitious and ceramic materials addresses the wake process zone responsible for the toughening characteristics evidenced by a rising R-curve behavior. New design philosophies incorporating principles of flaw tolerance require not only the quantitative evaluation of this process zone but an understanding of the mechanisms affecting the distribution and magnitude of cohesive stresses transferred, as well.

Several indirect methods have been advanced based on theoretical modelling studies to characterize the relationship between the bridging stresses and the crack opening displacement (COD) in the fracture process zone. Hillerborg et al. (1976), suggested a model for the analysis of initiation and propagation of cracks in concrete structures on similar lines of the Barenblatt (1962) and Dugdale (1960) model. In contrast to the single valued cohesive stress of a perfectly plastic metal, Hillerborg et al. (1976) proposed the existence of cohesive stresses which varied with crack face separation similar to the curve in Figure 1. This linear relationship between stress and COD is one of the possibilities offered by the authors. However, this was found to be in reasonable agreement with the already existing data on strain softening at that time (Evans and Marathe, 1968). Wecheterana and Shah (1983) applied a similar concept to model the post-peak response in fiber reinforced concretes according to the relationship,

$$\sigma/\sigma_{max} = (1-u/u_{max})^m, \quad (1)$$

where, u = crack opening displacement, σ = post-cracking stress and m is the strain softening exponent equal to 2.

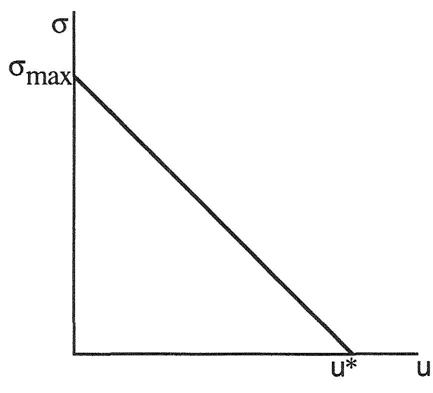

Fig. 1. Variation of stress with crack-width as proposed by Hillerborg et al. (1976).

Mai and Lawn (1987) and Foote et al. (1986) have discussed several possible connections between the strain softening exponent and the bridging mechanism, for different types of materials like fiber reinforced composites, concretes and ceramics. In concrete and ceramics, the falling tail portion of the stress-displacement curve originates from the stable separation of interlocking grains in these materials. Mai and Lawn (1987), adopted the same power law function for cementitious and ceramic materials, where m is an exponent which determines the contribution of the microstructure to the wake. In their work, they suggest that m=0 for a uniformly distributed stress over the bridging zone, m=1 for frictional pullout of the bridging grains and m=2 for fibrous composite materials.

Wittmann and Hu (1990, 1991) and Wittmann (1992) introduced a feasible method for the estimation of the crack tip bridging stresses in mortar and concrete. This method comprises of stepwise renotching of an extended crack and measuring the change in compliance between each saw cut. With each successive removal of the wake region, they observed a gradual increase in compliance which eventually became equal to the linear-elastic compliance by complete removal of the wake. This procedure was similar to the renotching experiments of Knehans and Steinbrech (1982), except that Hu and Wittmann (1991) used incremental cutting steps to extract information regarding the distribution of wake tractions. Assuming a linear crack profile, they went on further to estimate the distribution of the bridging stresses, as the increment of compliance due to multicutting is directly related to the above mentioned stresses. An analytical method to determine the modified compliance and hence bridging stress distribution has also been shown in their work assuming the validity of equation (1). A knowledge of bridging stress and compliance enabled them to model a K_R curve based on fracture energy G_f (involved in the process zone) and also to predict analytically the entire history of the bridging zone development.

Foote et al. (1986) have also proposed a theoretical model for calculating the crack growth resistance curves of strain softening cementitious materials. As the crack closure forces and crack opening displacements are interrelated, these workers have used an iterative scheme for K_R curve calculation using Castigliano's theorem for finding the relationship between COD and stress-intensity factors due to applied and bridging loads. They further proposed an approximate solution for K_R using linear-crack opening profile. The reasonably good matching between the exact and approximate solutions showed that the crack profile within the process zone is insensitive to the distribution of the bridging stresses transferred, supporting the assumption of a linear crack opening profile used by Hu and Wittmann (1991) in their models. This concept of a linear crack profile and the power law of equation (1), has been assumed for various structural materials where the softening coefficient, m, has been used to characterize the different toughening mechanisms.

Most of the above research on the study of the wake zone in cementitious materials is focussed on R-curve modelling based on theoretical stress-displacement relationships and determining the extension of the process zone and its dependance on the specimen geometry and size. A literature survey reveals that there have been some efforts on experimental determination of the strain softening relationship (Evans and Marathe, 1968; Peterson, 1981; Gopalarathnam and Shah, 1985; and Cornellison et al., 1986) with different degrees of success. Gopalarathnam and Shah (1985), attempted to experimentally identify the softening response of plain concrete in tension using double-edge-notched beam specimens. In situ optical observations revealed that a single crack formed across the specimen width just after the peak tensile load. Assuming zero crack width at peak stress level, they analytically modelled the post-peak strain softening response. A similar approach has been adopted by Cornellison et al. (1986), to determine fracture mechanics parameters in normal and lightweight concrete.

Li et al. (1987), suggested an indirect method to experimentally determine tension-softening curves in mortar. They derived a relation between stress and crack-tip separation from the J-Integral approach, by which the strain softening curve could be deduced by experimentally measuring the load, load-point displacement and the crack tip separation for two CT specimens with different starter notch lengths. These experimental studies provide a basis for FPZ characterization but fall short of directly measuring the bridging stress-COD relationship without the help of any assumptions.

To measure the actual crack bridging forces in ceramics experimentally, Reichl and Steinbrech (1988) adapted the short double cantilever beam specimen modified with a short backnotch, supported by a wedge. A non-catastrophic load drop occurred as the crack entered the rear notch. From the single value of an applied load and an average COD condition, a wake stress was calculated. Hay and White (1992 and 1993), developed the first experimental technique for direct experimental measurement of the bridging stress-crack opening displacement distribution in monolithic alumina and magnesium aluminate spinel structures. In contrast to the Reichl and Steinbrech (1988) work which only considered one stress evaluated from one COD condition, the bridging stress actually decays rapidly with increasing crack face separation due to the reduction in the number of active grains bridging the larger CODs in that region. In Figure 2, a schematic illustrates the decreasing stress with increasing COD. In the method proposed by Hay and White, post fracture tensile (PFT) specimens were

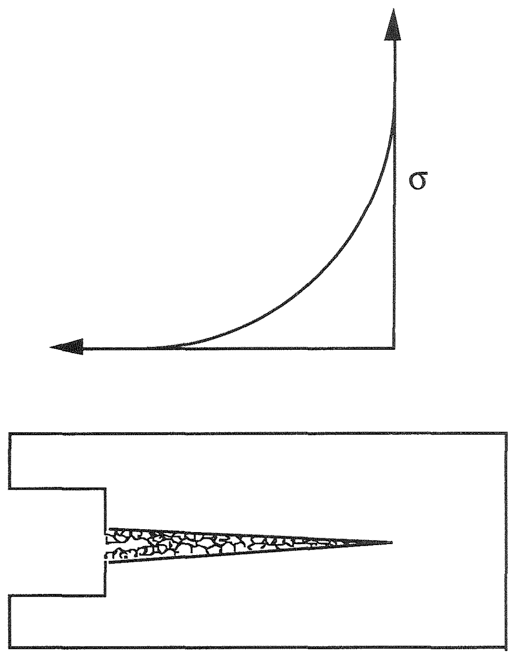

Fig. 2. Schematic view of the grain-bridging mechanism.

cut from behind the crack tip of a damaged DCB specimen and these isolated sections were loaded in tension to obtain the bridging stress distribution as a function of increasing COD behind the crack tip.

The PFT results for different grain-size specimens were correlated with the microstructure by making an analysis of the grain-size distributions. The COD/grain-size criteria, (β=COD/grain size) quantifies the amount of physical overlap required for grain bridging

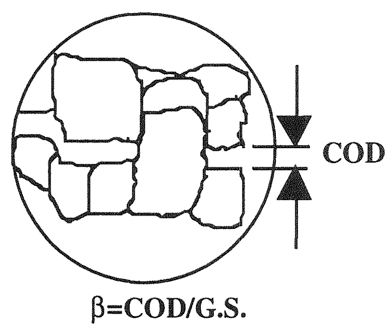

Fig. 3. Physical significance of the bridging efficiency factor, β. Here, negligible loads may be carried by grains even though overlap is apparent.

and is shown schematically in Figure 3. Although there is some physical overlap of the larger grains apparently seen in Figure 3, they cannot take part in the load sharing event unless they meet the COD/grain-size(β) criteria, and this concept was used by Hay and White to model the PFT curve. Fitting of the modelled PFT curves with the experimentally determined results provide an estimate of the interlocking parameter, β. Details of this technique are given by Hay and White (1993).

Application of the PFT technique to DCB specimens provides R-curve characterization (Hay and White, 1994), as R-curves obtained from this specimen geometry are independent of notch depth unlike those obtained from bend bars which depend heavily on initial crack length. Consideration of the stress-displacement relationship by Hay and White (1992) led to a model of the R-curve, which accounts for the fracture energy consumed in the wake. This can be obtained by the area under the extrapolated PFT stress-displacement curve and integrating this over the entire crack extension assuming linear crack profiles. Comparison of the modelled G_R curve (from PFT results) with the experimentally determined ones (from DCB specimens) showed good agreement, validating their approach to wake zone characterization.

The present approach is an application of the above novel technique developed by Hay and White (1992, 1993 and 1994) for wake zone characterization and R-curve modelling to concrete structures. This approach will lead to a more comprehensive knowledge of the detailed mechanism of the wake zone toughening process. Here, we correlate the bridging stresses directly with microstructural constituents including sand or aggregate in the concrete.

Experimental Procedures

The mix proportion of the concrete used in this study is given in Table 1. The quantities shown indicate the weight of each of the constituents (gms.) added per unit volume of the cast concrete (cm^3). The concrete mix was cast in 150 mm x 51 mm x 25 mm plate form and cured in a humid room (100 % relative humidity at 23°C) for 21 days. A polished sample, shown in Figure 4, shows the size, morphology and spatial arrangement of the grains. Specimen preparation for the optical micrographs included polishing with coarse to fine silicon carbide paper on a Vibromet wheel and a final polish with 5 μm diamond paste. The average aggregate size determined from Figure 4, is approximately 600 μm. A detailed analysis of the grain-size distribution appears in a following section. The shape of the sand grains retained in a no.30 sieve

Table 1. Material Composition of mortar used in the present investigation.

Cement Type	Portland Cement
Aggregate Type	Type 2 Blasting Sand (0.6 mm nominal grain size)
Water / Cement Ratio	0.4
Cement	0.797 gm/cm^3
Sand	1.594 gm/cm^3
Water	0.32 gm/cm^3
Age	21 days

(grains greater than 600 μm) were analyzed in the SEM (Figure 5) and compared with the standard chart for making an evaluation of aggregate shapes provided by Ozol (1978). From Figure 5, most of the sand grains appear to be semi-angular to semi-roundish in shape.

The DCB specimen geometry was selected for testing for two reasons. First, the small COD profile required for the PFT test is more easily obtained from a long crack than from the short crack associated with a bend bar. Secondly, the R-curves for the bend-bar specimens are sensitive to initial crack length. The DCB specimens were cut with a diamond slicing blade with a hydraulically driven surface grinder from the above plates where the specimen dimensions are (Figure 6), L=145

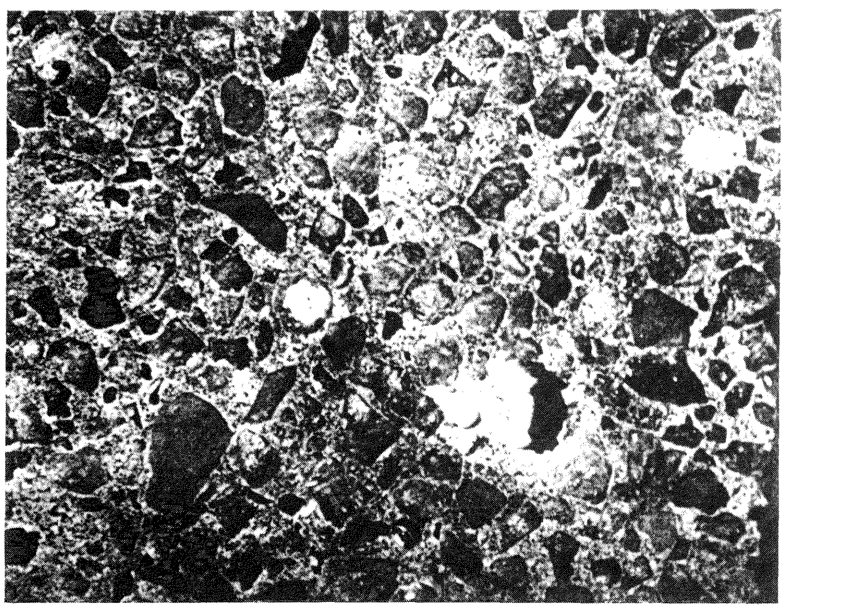

Fig. 4. Polished sample of the mortar specimen.

mm, a_o=50.8 mm, h=25.2 mm, w=12.7 mm, w'=6.35 mm, t=3.81 mm. The side grooves in the DCB specimens as shown in Figure 6, were introduced to ensure that the crack remained in plane. Four specimens of this size were tested.

The fracture tests were carried in the Instron testing machine using a crosshead speed of 2.5 µm/min. Upon completion of the DCB fracture test, the crack tip location was confirmed using an optical microscope. The DCB fracture test provided for a crack length of 35-40 mm. Load-displacement records were used to determine elastic-equivalent crack lengths by the compliance technique. The stress intensity factors for crack extension was evaluated as a function of crack length by (Kanninen, 1974; Srawley and Gross, 1967)

$$K_{Ri} = P_i\, a_i\, Y_i \,/\, bh^{1.5}, \qquad (2)$$

where, P_i is the instantaneous load, a_i is the corresponding crack length, b is the effective thickness (With, 1989) given by $(ww')^{1/2}$ and h is the specimen height.

In addition to the crack stabilizing side groove in the DCB specimens, two parallel grooves are machined These grooves accommodate the PFT loading fixtures, such that the load points align with the center of the cracked ligament. Thin slices, 3.81 mm thick,

Fig. 5. SEM photographs showing the roundish shape of the sand grains.

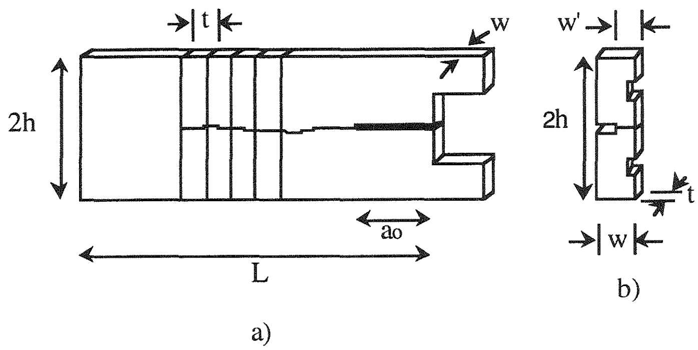

Fig. 6. Schematic of DCB and PFT specimen. a) Fractured DCB b) PFT specimen.

were extracted from the wake region (as indicated in Figure 6) to form the PFT specimens. The DCB specimen was secured to a steel substrate using a thermal glue (brittle at room temperature) to avoid damage to the wake during the slicing step. Since the peak stress and stiffness of a PFT curve depends on initial CODs, the starting crack face separation was measured for all PFT specimens.

Results and Discussion

The K_R data were compiled from the load displacement data obtained from the DCB tensile tests and have been shown in Figure 7. The K_R data can be broken down into a crack tip component and a wake component given by

$$K_R = K_i + \Delta K, \tag{3}$$

where, K_i is the initial point on the R-curve representing the crack tip resistance and ΔK is the shielding component due to the wake zone tractions. The point on the R-curve where the K_R values plateau indicates a fully saturated bridging zone which travels with the crack tip. Figure 7 shows that the bridging zone length exceeds 35 mm, but the ΔK toughening component is quite low when compared with other materials like structural ceramics (Hay and White, 1994). This indicates not only a low inherent toughness, but a low grain bridging efficiency, as well.

PFT specimens were loaded in tension at a crosshead speed of 2 μm/min to obtain load-displacement data. The load was divided by the cross-sectional area of the fractured region of the PFT specimen to obtain the bridging stresses and the initial displacements were shifted to

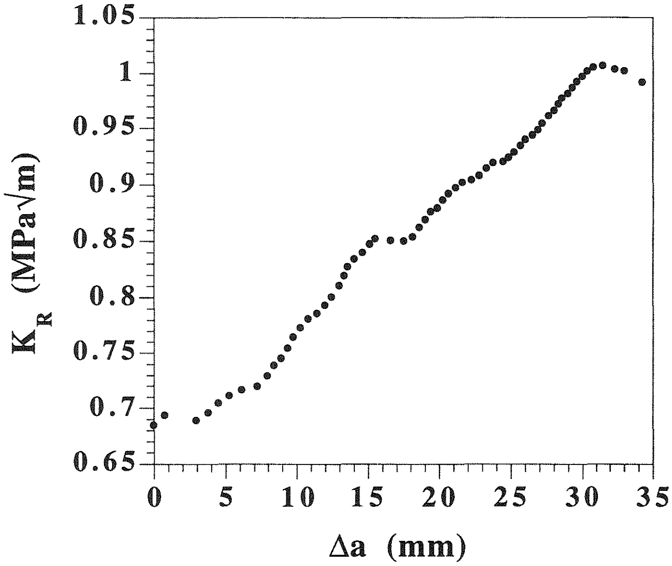

Fig. 7. Crack growth resistance curve (K_R) compiled from load-displacement data of DCB fracture test.

account for the residual CODs from the DCB fracture test. The resultant stress-displacement data of one PFT test is shown in Figure 8. The stress-displacement curve contains four distinct behavioral regions. An apparent linear-elastic region characterizes the behavior for loads below approximately 90% of the maximum tensile stress suggesting minimal nonrecoverable movement. Just prior to critical conditions, there exists a short nonlinear region indicating nonrecoverable grain activities. Beyond the maximum load, the load bearing capacity of the process zone decreases monotonically due to increased crack-face separation ultimately approaching a negligible constant load.

The COD profile increases from zero at the crack tip to a maximum at the crack mouth near the chevron notch. The grains which satisfy the COD/grain-size criteria ($<\beta$) participate in the load sharing event and are called active grains. The increasing COD away from the crack tip corresponds to a decrease in the population of active grains, eliminating the smaller categories and decreasing the bridging efficiency (Figure 2.). For any particular crack opening displacement (COD), the active grains (capable of effective bridging) are the ones which are greater than or equal in size to COD/β. Therefore, from Figure 2, it is clear that bridging is a maximum at the crack tip and a minimum at the crack mouth. From this analysis, it is evident that the strength and distribution of the tractions within the process zone depends on the grain-size distribution.

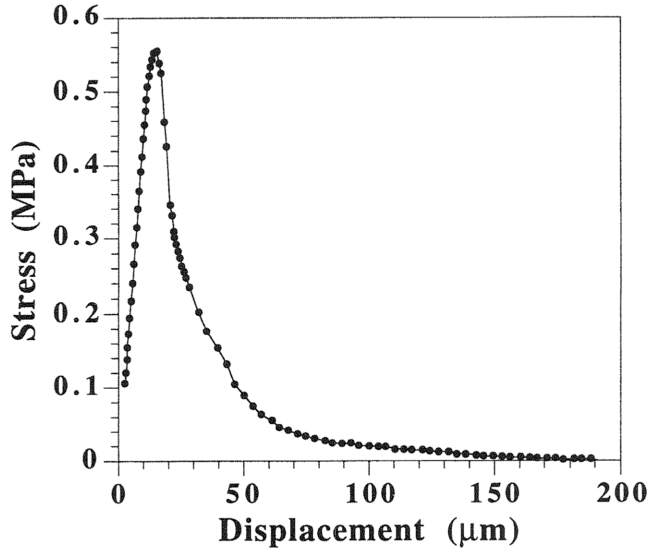

Fig. 8. Typical stress-displacement data for mortar, obtained from the PFT method.

To study this behavior in more detail, various PFT specimens with different starting CODs were tested in tension. Three such PFT results are shown in Figure 9. The lower curve, corresponding to the largest COD profile, indicates the lower bridging stresses expected from a smaller population of active bridging grains in the process zone farthest from the crack tip. The greater damage characterized by the larger COD and lower bridging grain population results in a reduction of both the elastic stiffness and the peak stress. As the starting COD is reduced, the larger population of bridging grains as well as the improved contact results in higher peak stresses and increased elastic stiffness as shown in the upper curves. The agreement between the advanced stages of the strain softening curves where equivalent CODs overlap is of considerable significance. This shows that the strain-softening segment of the PFT curves is related to the development of a characteristic fracture process in the wake.

A curve fit to the envelope described by the family of PFT curves is shown in Figure 9. The stress-axis intercept of this curve fit indicates the stress required to open a crack of zero COD (the fictitious stress required to separate a crack without any opening but in which the physical bonds have already been broken). This extrapolated curve describes the bridging stress-COD relationship in the FPZ. For the particular concrete tested, this yields a critical stress (σ^*) of 0.5 MPa. and a critical COD (u^*) of around 140 µm. This value of the critical COD obtained is comparable to data available in the literature (Hu and

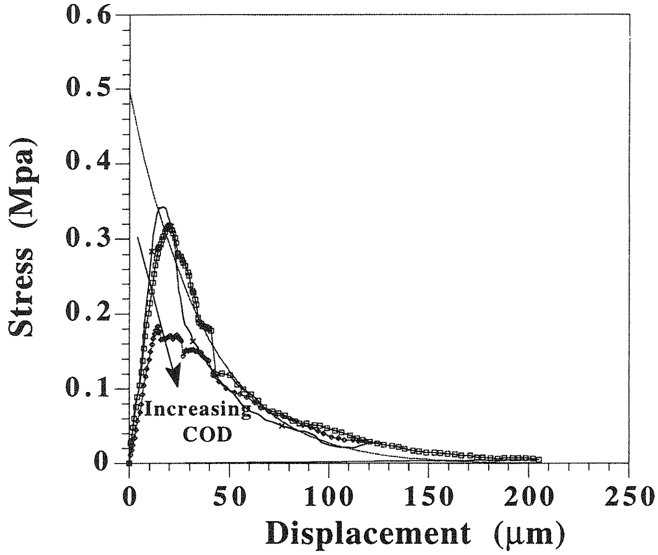

Fig. 9. Family of stress-displacement curves from PFT specimens with different initial CODs. A curve fit of the experimental data estimates the stress-displacement relationship.

Wittmann ,1991), but the critical stress is less than the data available in the literature. Two theories may explain this discrepancy. The critical stress obtained in this work represents the stress to open a crack of zero COD, where those reported in the literature are the tensile strengths of the materials. Second, since the composition and nominal grain size of our samples are different from the ones reported in related works, one would expect effects on both the critical stress and limiting COD.

Microstructure

In Figure 10 fractographs from mating fracture surface areas evidence a predominantly intergranular fracture characterized by a rough fracture surface where grain pullout has occurred. This indicates that almost 100% of the grains can take place in the load-sharing event in the process zone, provided they meet the COD/grain-size criteria.

The grain-size distribution of the concrete sample considered in this study was determined from polished specimens. All grains were optically measured for their long and short dimensions from optical photographs and the grain area was calculated assuming an elliptical morphology. The grain size reported is the equivalent diameter of these elliptical grains with the same cross-sectional area. The grain sizes are

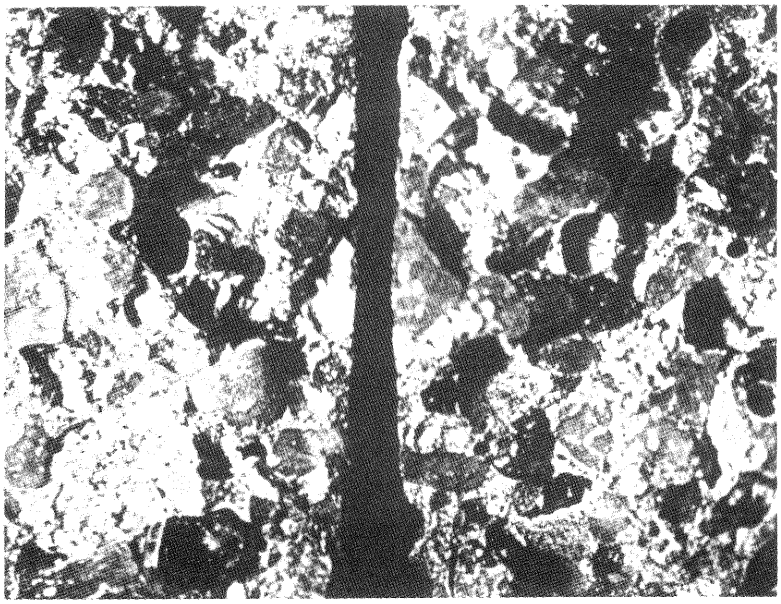

2 mm

Fig.10. Fractographs of mating fracture surface areas showing predominantly intergranular fracture.

categorized in 100 μm intervals and presented in Figure 11. To relate the effects of the grain size to stress-displacement curves, the area fraction occupied by each grain-size category has been plotted. For the present material, majority of the area is occupied by grains ranging from 300 μm to 900 μm in diameter, and the average grain size is approximately 550 μm.

The microstructural influence on the stress displacement curve is analyzed by assessing a COD/grain size(β) criteria which quantifies the amount of physical overlap required for bridging. An assumption is made that the same β factor applies to all grain sizes. The active area fraction for any given COD is calculated by integrating the data in Figure 11, from 1/β times the COD to the maximum grain size. Repeating this for the entire rage of CODs results in a relationship describing the active contact area versus displacement. The area fraction versus displacement relationship is then multiplied by the critical stress, 0.5 MPa and a modelled PFT stress-displacement relationship is obtained as shown in Figure 12. If all grain sizes possess the same critical stress of 0.5 MPa, then the curve in Figure 12 should possess the same shape as the PFT curve. Comparison of the modelled curves with the experimentally determined PFT curves shows that a β value of 1/15 to 1/16, gives good agreement with the extrapolated PFT curve. This value of β is considered to be very low compared with those obtained for

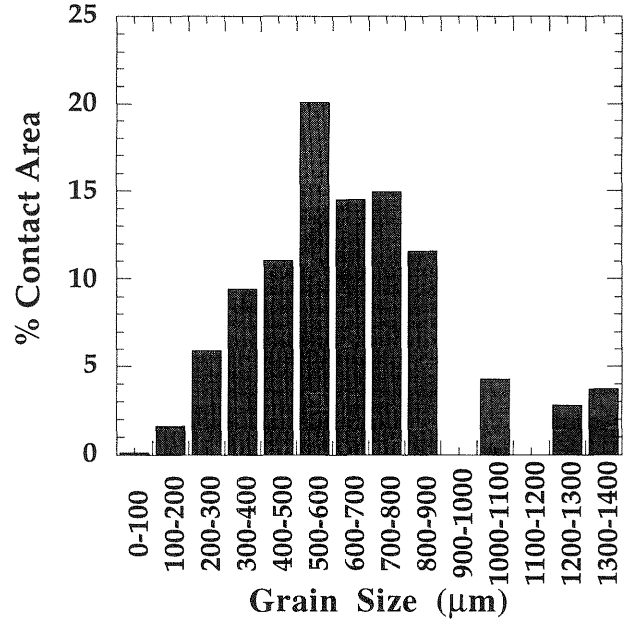

Fig. 11. Grain-size distribution for the mortar specimen.

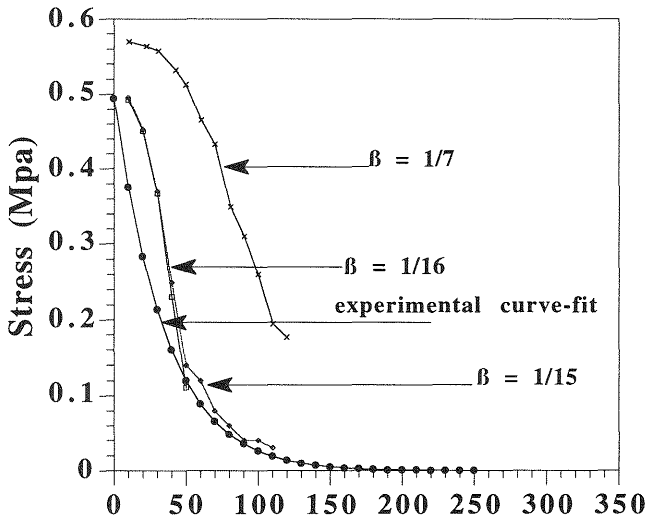

Fig.12. Modelled stress-displacement curve determined from grain-size distribution and the power-law curve fit to experimental data.

ceramics (Hay and White,1994; Kelkar and White, 1990; Steinbrech et al., 1988), signifying a lower grain bridging efficiency in the mortar specimen. Bridging of grains depends on both geometrical and elastic interactions between the sand grains and the surrounding cement matrix. Increases in the angularity of the grains (Mantuani, 1983), addition of silica fumes to the microstructure (Tasedemir, Grimm and Konig,1995) and other compositional variables are, therefore, expected to increase the bridging efficiency. The sand grains used in this study are mostly semi-rounded to semi-angular and may have contributed to the low peak bridging loads and efficiency described by β.

Conclusions

The novel post-fracture tensile (PFT) technique is a valuable experimental method to directly measure the grain bridging stresses in the wake zone of cementitious materials such as concrete and mortar. The reasonably good agreement of the critical COD value derived from PFT testing with data reported in the literature gives us more confidence in the application of this experimental method in determining the fracture mechanics parameters of concrete-like material. Microstructural characterization of the specimen gives an indication of the grain bridging efficiency (β), which was found to be low in our case compared with ceramic materials for which this technique has been applied. Further investigations are being carried out to understand the effect of technical parameters like aggregate size, shape (angularity), composition of mortar etc., on the stress-COD curve and the bridging efficiency factor.

References

Barenblatt, G.I.(1962) The mathematical theory of equilibrium cracks in brittle fracture. **Adv. App. Mech.,** 6, 55-129.

Cornellison, H.A.W., Hordijk, D.A. and Reinhardt, H.W. (1986) On experiments and theory for the application of fracture mechanics to normal and lightweight concrete, in **Fracture Toughness and Fracture Energy of Concrete** (eds. F.H.Wittmann), Elsevier, New York, 565-576.

Dugdale, D.S. (1960) Yielding of steel sheets containing slits. **J. Mech. Phys. Solids,** 8, 100-108.

Evans, P.H. and Marathe M.S.(1968) Microcracking and stress-strain curves for concrete in tension. **Mat. and Struct. (RILEM),** 1, 61-64.

Foote,R.L., Mai, Y.W. and Cottrell, B. (1986) Crack growth resistance curves in strain softening materials. **J. Mech. Phys. Solids,** 34, 593-607.

Gopalarathnam, V and Shah, S.P. (1985) Softening response of plain concrete in direct tension. **ACI journal,** 82, 310-323.

Grimes, R.E., Kelkar, G.P., Guazzone, L. and White, K.W. (1990) Elevated temperature R-Curve of a polycrystalline alumina. **J. Am. Ceram. Soc.,** 73, 1399-1404.

Hay, J.C. and White, K.W. (1992) Crack face bridging mechanisms in monolithic $MgAl_2O_4$ spinel microstructures. **Acta Met. Mat.,** 40, 3017-3025.

Hay, J.C. and White, K.W. (1993) Grain bridging in monolithic alumina and spinel. **J. Am. Ceram. Soc.,** 76, 1849-1854.

Hay, J.C. and White, K.W. (1994) Effect of thermoelastic anisotropy on the R-Curve behavior of monolithic alumina. **J. Am. Ceram. Soc.,** 77, 2283-2288.

Hillerborg, A., Modeer, M. and Petersson, P.E.(1976) Analysis of crack formation and crack growth in concrete by means of fracture mechanics and finite elements. **Cem. and Con. Res.,** 6, 773-782.

Hu, X.Z., Lutz, E.H. and Swain, M.(1991) Crack-tip bridging stresses in ceramic materials. **J. Am. Ceram. Soc.,** 74, 1828-1832.

Kanninen, M.F.(1974) A dynamic analysis of crack propagation and arrest in the DCB test specimen. **Int. J. Fract.,** 10, 415-430.

Kelkar, G.P. and White, K.W. (1991) Evaluation of the crack face bridging mechanism in a $MgAl_2O_4$ spinel. **J. Am. Ceram. Soc.,** 74, 1732-1734

Knehans, R. and Steinbrech,R.(1982) Memory effect of crack resistance during slow crack growth in notched alumina bend specimens. **J Mat. Sci. Lett.,** 1, 327-329.

Li, V.C., Chan, C.M. and Leung,C.K.Y.(1987) Experimental determination of the tension softening relations for cementitious composites. **Cem. and Con. Res,** 17, 441-452.

Mantuani, L.D.(1983) On properties of concrete aggregates, in **Handbook of concrete aggregates - a petrographic and technological evaluation**, Noyes Publ., New.Jersey., 24-50.

Mai, Y.W. and Lawn, B.R.(1987) Crack-Interface grain bridging as a fracture resistance mechanism in ceramics: II, Theoretical fracture mechanics model. **J.Am Ceram. Soc.,** 70, 289-294.

Ozol, M.A. (1978) Shape, surface texture, surface area and coatings. **ASTM STP.,** 169B, 584-628.

Peterson, P.E.(1981) Crack growth and development of fracture zones in plain concrete and similar materials. **Report TVBM-1006, Lund Institute of Technology, Division of Building Materials.**

Reichl, A. and Steinbrech, R.W. (1988) Determination of crack-bridging forces in alumina. **J. Am. Ceram. Soc.,** 71, C299-C301.

Srawley, J.E. and Gross, B.(1967) Stress intensity factors for crack line-loaded edge-crack specimens. **Materials Res. and Stand.,** 7, 155-162.

Wecharatana, M and Shah, S.P.(1983) A model for predicting fracture resistance of fibre reinforced concrete. **Cem. and Con. Res.,** 13, 819-829.

With,G. (1989) Small specimen double cantiliver-beam test applicable to monolithics and joints. **J. Am. Ceram. Soc.,** 72, 710-712.

Wittmann, F.H. and Hu, X.(1990) Experimental method to determine extension of fracture process zone. **J. of Mat. in Civil Engg.,** 2, 15-23.

Wittmann, F.H. and Hu, X.(1991) Fracture process zone in cementitious materials. **Int.J.of Fract.,** 51, 3-18.

Wittmann, F.H. and Hu, X.(1991) An analytical method to determine the bridging stress transferred within the fracture process zone I, General theory. **Cem. and Con. Res,** 21, 1118-1128.

Wittmann, F.H. (1992) On Fracture process zone and fracture energy. **Fracture mechanics of concrete structures** (eds. Z.P.Basant), FramCOS 1, Elsevier applied science, 391-403.

Tasedemir, C.,Tasedemir, T.A., Grimm, R. and Konig G.(1995) Microstructural effects on the brittleness of high strength concrete. **Proc. of the 2nd. int. conference on fracture mechanics of concrete structures (FramCOS 2)** (ed. F.H.Wittmann), Aedificatio pub., Freiburg, Germany, 125-134.